Regulation of Vertebrate Cellular Mg^{2+} Homeostasis by TRPM7

Carsten Schmitz,[1,6,7] Anne-Laure Perraud,[1,2,6]
Catherine O. Johnson,[1] Kazunori Inabe,[3]
Megan K. Smith,[1] Reinhold Penner,[5]
Tomohiro Kurosaki,[3,4] Andrea Fleig,[5]
and Andrew M. Scharenberg[1,*]
[1]Department of Pediatrics
Department of Immunology
University of Washington and
Children's Hospital and Regional Medical Center
Seattle, Washington 98195
[2]Department of Immunology
National Jewish Medical and Research Center
Denver, Colorado 80206
[3]Department of Molecular Genetics
Institute for Liver Research
Kansai Medical University
570-8506 Osaka
Japan
[4]Laboratory for Lymphocyte Differentiation
RIKEN Research Center for Allergy and Immunology
570-8506 Osaka
Japan
[5]Laboratory of Cell and Molecular Signaling
Center for Biomedical Research at The Queen's
  Medical Center and John A. Burns School
  of Medicine at the University of Hawaii
Honolulu, Hawaii 96813

Summary

TRPM7 is a polypeptide with intrinsic ion channel and protein kinase domains whose targeted deletion causes cells to experience growth arrest within 24 hr and eventually die. Here, we show that while TRPM7's kinase domain is not essential for activation of its channel, a functional coupling exists such that structural alterations of the kinase domain alter the sensitivity of channel activation to Mg^{2+}. Investigation of the relationship between Mg^{2+} and the cell biological role of TRPM7 revealed that TRPM7-deficient cells become Mg^{2+} deficient, that both the viability and proliferation of TRPM7-deficient cells are rescued by supplementation of extracellular Mg^{2+}, and that the capacity of heterologously expressed TRPM7 mutants to complement TRPM7 deficiency correlates with their sensitivity to Mg^{2+}. Overall, our results indicate that TRPM7 has a central role in Mg^{2+} homeostasis as a Mg^{2+} uptake pathway regulated through a functional coupling between its channel and kinase domains.

Introduction

TRPM7 is a member of the TRPM family of cation channels (Clapham et al., 2001; Elliott, 2001; Harteneck et

*Correspondence: andrewms@u.washington.edu
[6]These authors contributed equally to this work.
[7]Present address: Department of Immunology, National Jewish Medical and Research Center, Denver, Colorado 80206.

al., 2000; Hofmann et al., 2000; Montell et al., 2002), a recently described ion channel family defined by a constellation of features consisting of a large conserved N-terminal region, an adjacent cation channel transmembrane spanning region, and a short nearby region of high coiled coil character (reviewed in Clapham et al., 2001; Montell et al., 2002; Vennekens et al., 2002). The C-terminal domain distal to the coiled coil region varies significantly between different TRPM family members. Within the TRPM family, TRPM6 and TRPM7 are notable in that they contain protein kinase domains within their unique C-terminal sequences. In contrast to TRPM2, where a C-terminal nudix hydrolase domain has been clearly implicated in channel activation (Hara et al., 2002; Perraud et al., 2001; Sano et al., 2001; Wehage et al., 2002; reviewed in Perraud et al., 2003), the relevance of TRPM7's kinase domain to channel function remains controversial (Nadler et al., 2001; Runnels et al., 2001): TRPM7 channel activation has been suggested to be dependent on the phosphotransferase activity of the intrinsic kinase domain (Runnels et al., 2001), while suppression of activation/channel deactivation has been shown to occur in response to Mg^{2+}-nucleotide complexes or Mg^{2+} alone (Nadler et al., 2001; Runnels et al., 2002), G protein activation (Hermosura et al., 2002), and PIP$_2$ hydrolysis (Runnels et al., 2002). In addition, conflicting data have been presented regarding TRPM7 channel permeation characteristics, with data suggesting both nonselective conduction of Na$^+$ and Ca^{2+} (Runnels et al., 2001) and complex permeation with selectivity toward divalent cations (Monteilh-Zoller et al., 2003; Nadler et al., 2001).

In order to gain a better understanding of the cell biological role of TRPM7, we investigated the relationship between cellular Mg^{2+} and the channel and kinase functions of TRPM7 using a combination of electrophysiological, biochemical, and genetic approaches. Our results indicate that TRPM7 serves as an essential Mg^{2+} uptake pathway regulated through a functional coupling between its channel and kinase domains.

Results

Changes in Free Mg^{2+} Produce Correlated Changes in TRPM7 Channel and Phosphotransferase Activities

As TRPM7 channel activation has been suggested to require an active kinase domain (Runnels et al., 2001), and we have previously demonstrated that Mg^{2+}/Mg·ATP are two factors involved in setting TRPM7 channel activity (Nadler et al., 2001), we therefore analyzed the relationship between free [Mg^{2+}], whole-cell TRPM7 currents, and TRPM7 in-vitro phosphotransferase activity. Using hTRPM7 in-vitro autophosphorylation as a readout of phosphotransferase activity, provision of even 1 mM free [Mg^{2+}] under standard in vitro assay conditions produced a substantial enhancement of wild-type (WT) hTRPM7 phosphotransferase activity (Figure 1, left). As physiological levels of intracellular free [Mg^{2+}] are
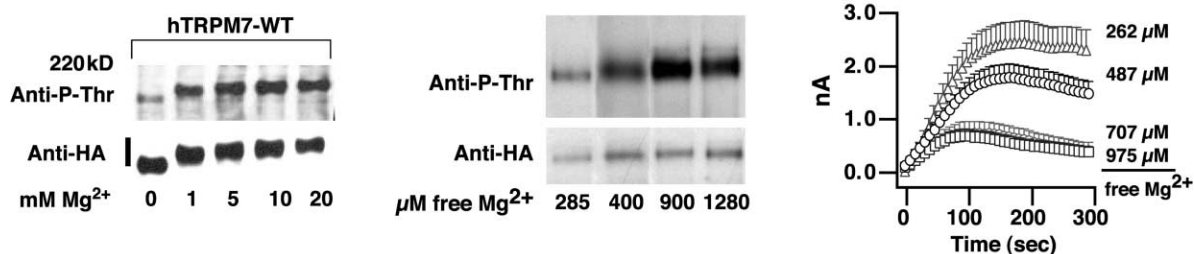
Figure 1. Mg^{2+} Mediates Correlated Changes in TRPM7 Channel Domain Gating and Kinase Domain Phosphotransferase Activity

Left: Mg^{2+} enhances phosphotransferase activity in immunoprecipitates of wild-type TRPM7. Middle: in vitro kinase analysis of WT HA-TRPM7 activity at varying free Mg^{2+} as indicated and constant total 5 mM Mg·ATP. Right: whole-cell patch clamp analysis of WT HA-TRPM7 currents at varying free Mg^{2+} and fixed 5 mM Mg·ATP. Plots represent n = 9, 13, 7, 11 experiments (262, 487, 707, 875 μm free Mg^{2+}, respectively).

thought to be in the range of 0.5–1.0 mM and physiological concentrations of intracellular ATP are thought to be in the range of 2–6 mM, we analyzed hTRPM7 phosphotransferase activity and hTRPM7 channel function under conditions in which [Mg·ATP]i concentrations were held at 5 mM while free [Mg^{2+}]i was varied (Figure 1, middle and right). As can be seen in the middle, varying free [Mg^{2+}]i over a range of 285–1200 μM produces graded changes in hTRPM7 in vitro phosphotransferase activity. Similarly, varying free [Mg^{2+}]i between approximately 250 μM and 1 mM in whole-cell patch clamp experiments produces graded suppression of hTRPM7 channel function (right). Thus, changes in free [Mg^{2+}]i within the putative physiologic range result in correlated changes in the activation of hTRPM7 channels and hTRPM7 kinase domain phosphotransferase activity, consistent with the existence of a functional relationship between the kinase and channel functions of TRPM7.

TRPM7 Phosphotransferase Activity-Deficient Point Mutants Activate Fully in Response to Decreased Free Mg^{2+}/Mg·ATP

Knowledge of TRPM7 structure/function relationships is presently insufficient to allow the design of mutants specifically defective in channel opening. However, the crystal structure of the TRPM7 kinase domain has been determined in isolation, allowing amino acid residues required for phosphotransferase activity to be unambiguously identified (Yamaguchi et al., 2001). Therefore, we initiated an experimental investigation of the relationship between the kinase and channel domains of TRPM7 through analysis of mutant proteins defective in phosphotransferase activity. Using information from the crystal structure, we constructed two distinct human TRPM7 (hTRPM7) phosphotransferase activity-deficient point mutants (see schematic in Figure 2A, expression Figure 2B left panel), and analyzed them for alterations in their channel function. The relative phosphotransferase activities of the WT hTRPM7 channel and mutants were analyzed by an in vitro autophosphorylation assay, which demonstrated easily detectable phosphotransferase activity of the WT channels and much reduced to absent activity of the mutant channels under standard conditions (Figure 2B, right). Whole-cell patch-clamp analysis of the channel properties of the WT, G1799D, and K1648R hTRPM7 proteins showed that with nominal zero intracellular Mg^{2+} pipette solution (which produces

maximal activation of WT murine TRPM7 [mTRPM7] [Nadler et al., 2001]), the G1799D and K1648R phosphotransferase-activity deficient mutants activated to a similar extent as WT hTRPM7, with expression of each protein correlating with the development of whole-cell currents from 10- to 20-fold greater than those found in uninduced cells (current evolution is shown in Figure 2C top, respective I/V curves at maximal current magnitude [250 s] are shown at the bottom). Furthermore, overexpression of the WT hTRPM7 and both mutants induced cell death in HEK-293 cells in the same qualitative manner as described earlier for WT mTRPM7 (Nadler et al., 2001 and data not shown). From these data, we conclude that phosphotransferase activity is not required for TRPM7 channel activation. This conclusion is unexpected, as a previous analysis of mTRPM7 had found that a point mutation essentially identical to that in our G1799D human TRPM7 mutant (which destroys a conserved GxAxxG motif within the kinase domain activation loop) eliminated its channel domain's ability to activate, and this result was interpreted in favor of phosphotransferase activity-dependent activation of the TRPM7 channel (Runnels et al., 2001). The reason for the differences between our results and previous results remains unclear, as we excluded a species difference in requirement for phosphotransferase activity for channel activation by analyses of a fusion channel consisting of amino acids 1–1561 of murine TRPM7 fused to amino acids 1197–1503 of human TRPM2. Using this construct, which completely lacks the murine TRPM7 kinase domain, we have observed readily detectable activation of currents with the TRPM7 signature I/V curve under nominally 0 internal Mg^{2+} conditions (not shown).

TRPM7 Phosphotransferase Activity-Deficient Point Mutants Exhibit Deficient Mg^{2+}/Mg·ATP-Dependent Suppression of Channel Activity

We noted during the experiments above that whole-cell currents present just after break in were on average substantially greater for the kinase domain mutant channels (G1799D, 1.15 ± 0.24 nA, n = 10; K1648R, 0.95 ± 0.32 nA, n = 9) relative to WT TRPM7 (0.19 ± 0.10 nA, n = 8; currents at time 0 in Figure 2C), even though similar maximal current magnitudes were eventually achieved. This suggested that the G1799D and K1648R mutations might somehow be promoting channel activity. In order to better characterize this phenomena, we
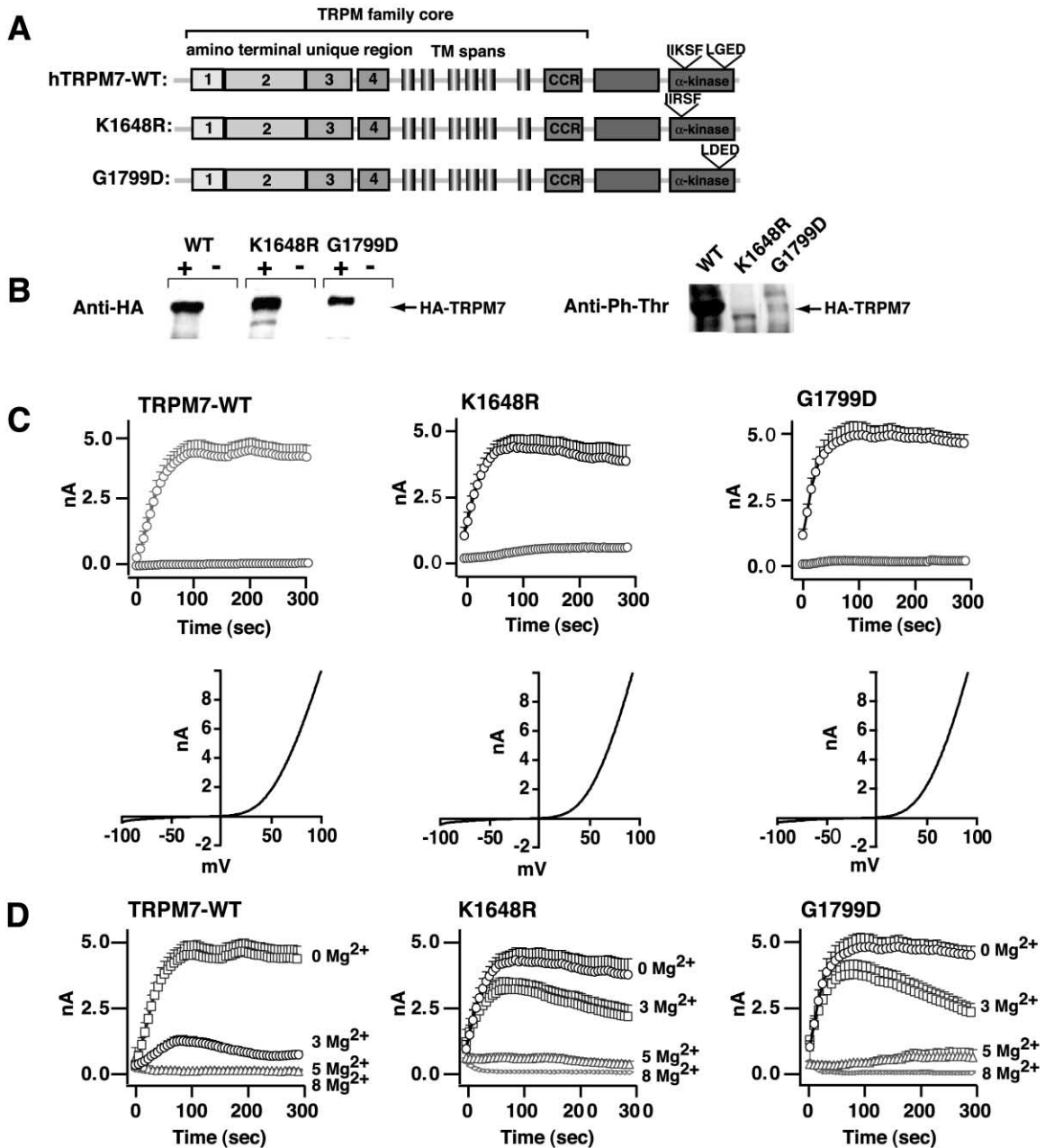
Figure 2. Analysis of Mg²⁺-Mediated Regulation of TRPM7 Phosphotransferase Activity-Deficient Point Mutants

(A) Schematic of TRPM7 and location of point mutations affecting TRPM7 kinase activity.

(B) Left: anti-HA immunoblot analysis of HEK-293 cells with doxycycline-regulated expression of human HA-TRPM7-WT and human HA-TRPM7 mutants. Abbreviations: +, doxycycline treated; −, untreated. Right: anti-phosphothreonine immunoblot analysis of in vitro kinase activity of HA-TRPM7-WT and the two HA-TRPM7 kinase-deficient point mutants.

(C) Whole-cell patch clamp analyses of currents produced after break in with nominal 0 Mg²⁺ pipette solution for HA-WT and HA-TRPM7 mutants. Top panels are current evolution with time. Plots represent $n = 9$ experiments (in), $n = 4$ (un) (TRPM7-WT); $n = 8$ experiments (in), $n = 10$ (un) (K1648R); and $n = 10$ experiments (in), $n = 4$ (un) (G1799D). Bottom panels are I/V curves at 300 s from representative experiments.

(D) Whole-cell patch clamp analysis of Mg²⁺ suppression of HA-TRPM7-WT and human HA-TRPM7 mutants. Pipette solutions contained the indicated concentrations of Mg²⁺. Plots represent $n = 9, 5, 4, 3$ experiments (TRPM7-WT, 0, 3, 5, 8 mM Mg²⁺, respectively), $n = 8, 5, 4, 3$ experiments (K1648R, 0, 3, 5, 8 mM Mg²⁺, respectively), and $n = 10, 9, 3, 3$ experiments (G1799D, 0, 3, 5, 8 mM Mg²⁺, respectively). Note 0 Mg²⁺ plots in (D) are the same plots as in (C).

evaluated Mg²⁺ and Mg·ATP-dependent suppression of channel activity (heretofore referred to as Mg²⁺/Mg·ATP suppression, respectively) of WT hTRPM7 and the two mutants over a range of Mg²⁺ and Mg·ATP concentra-

tions (Figure 2D). Strikingly, both phosphotransferase activity-deficient point mutant channels were significantly right shifted in their Mg²⁺/Mg·ATP suppression relative to WT hTRPM7 (compare Figure 2D, left, middle,

and right for Mg^{2+} suppression, data not shown for Mg·ATP suppression but summarized in dose-response curve in Figure 3D, right). These results lead to the conclusion that, while phosphotransferase activity is not required for channel activation, mutations that affect the phosphotransferase activity of the kinase domain do influence channel activity, supporting the concept of a functional coupling between TRPM7 channel and kinase domains.

A TRPM7 Kinase Domain Deletion Mutant Exhibits Enhanced Mg^{2+}/Mg·ATP-Dependent Suppression of Channel Activity

The K1648R and G1799D mutations are in regions of the hTRPM7 kinase domain, which are predicted to affect phosphotransferase activity by interfering with its ability to interact with Mg·ATP (Yamaguchi et al., 2001). Therefore, their effects on Mg^{2+}/Mg·ATP suppression could be due to the loss of phosphotransferase activity of the kinase domain or occur as a direct result of altered Mg^{2+} and ATP binding to the kinase domain. In order to test whether interactions between Mg^{2+}, Mg·ATP, and the kinase domain were directly involved in Mg^{2+}/Mg·ATP suppression of TRPM7, we evaluated the channel properties of a deletion mutant of human TRPM7 in which the entire kinase domain was removed following amino acid 1569 (TRPM7-Δ-kinase, see schematic Figure 3A, left, expression Figure 3A, right; TRPM7-Δ-kinase expression at the lysate level is similar to that of WT TRPM7, not shown). Consistent with our previous results from the point mutants, which established that phosphotransferase activity is not required for channel activation, the TRPM7-Δ-kinase channel was still functional, with induction of its expression correlating with the development of TRPM7-signature currents well above those of uninduced cells (Figure 3B left, I/V curve middle). However, analysis of Mg^{2+}/Mg·ATP suppression of TRPM7-Δ-kinase demonstrated that it is markedly more sensitive to both Mg^{2+} and Mg·ATP-mediated suppression than WT TRPM7, as nearly full suppression of channel activation occurred even at 1 mM Mg^{2+} (Figure 3B, right), or 1 mM Mg·ATP (data not shown but summarized in dose-response curve in Figure 3D, right), and expression of maximal channel activation required clamping internal Mg^{2+} to 0 with EDTA instead of using nominally 0 intracellular Mg^{2+} solutions (estimated [Mg^{2+}] 5 μM, Figure 3C, left, for both standard and divalent free (DVF) conditions with I/V curves shown at the right). While the somewhat smaller maximal currents observed with the TRPM7-Δ-kinase channel suggest that it may have slightly lower levels of surface expression and/or generally reduced open probability relative to WT hTRPM7, the fact that it is still capable of Mg^{2+} and Mg·ATP suppression provides unequivocal evidence that these phenomena are not only independent of the endogenous phosphotransferase activity of TRPM7, but also are apparently mediated by a structure entirely extrinsic to the kinase domain. In addition, the left-shifted Mg^{2+}/Mg·ATP suppression observed with TRPM7-Δ-kinase (quantitatively summarized along with the right shifted Mg^{2+}/Mg·ATP suppression of the TRPM7 phosphotransferase activity-dependent point mutants by the dose-response curves illustrated in Figure 3D), provides

further evidence that the TRPM7 kinase domain is somehow coupled to structures that regulate TRPM7 channel activity.

Supplementation of Extracellular Mg^{2+} Complements TRPM7 KO Phenotype and Corrects Mg^{2+} Deficiency in TRPM7-KO Cultured Cells

We have previously reported that TRPM7 permeates Mg^{2+} (Nadler et al., 2001). As our data above indicated that TRPM7 channel and kinase domains are functionally coupled so as to produce coordinated responses in their respective activities to changes in intracellular Mg^{2+}/Mg·ATP, we considered that TRPM7 might be directly involved in cellular Mg^{2+} homeostasis. We have also previously reported that cultured cells made deficient in TRPM7 via cre-lox-mediated destruction of the TRPM7 gene go into growth arrest and die after a few days in culture (Nadler et al., 2001). Since loss of an ion transport pathway resulting in a growth defect in lower eukaryotes and prokaryotes can often be complemented by supplementation of the ion transported by that pathway (Li et al., 2001; MacDiarmid and Gardner, 1998; Smith and Maguire, 1998), we evaluated whether the growth defect in TRPM7-deficient cells (KO cells) could be ameliorated to any extent by supplementing their growth media with Mg^{2+}. As illustrated in Figure 4A, left, provision of 10–25 mM supplemental Mg^{2+} (but not Ca^{2+}, Mn^{2+}, or Zn^{2+}) allowed inducible KO (iKO) cells to survive and grow in culture as well as their parental cell line. The supplemental Mg^{2+} did not affect the efficiency of conditional gene excision or stability of the TRPM7 mRNA (Figure 4A, right, and data not shown), indicating that it's growth supporting effect was through its ability to complement TRPM7 protein function. In addition, levels of supplemental Mg^{2+} between 1–10 mM showed a graded effect, with lower concentrations first supporting cell viability and higher concentrations gradually supporting faster rates of cell proliferation (not shown). This effect was specific to Mg^{2+} in that only Mg^{2+}-containing salts complemented, and both $MgSO_4$ and $MgCl_2$ complemented TRPM7-deficiency equally well (not shown). The iKO cells receiving Mg^{2+}-supplemented medium appeared morphologically normal in all respects and were able to grow like their parental cells as long as they were maintained in high levels of extracellular Mg^{2+}; when the supplemental Mg^{2+} was withdrawn, they rapidly went into growth arrest and eventually died over the next 48–72 hr. We were curious whether the Mg^{2+}-dependent growth defect in the iKO cells was responsible for our inability to produce a constitutive TRPM7-deficient line by a standard targeting strategy (Nadler et al., 2001). Therefore, we attempted to stably target the second TRPM7 allele in a TRPM7 heterozygote DT-40 line using media supplemented with 10 mM Mg^{2+}. This approach was successful in producing several TRPM7-deficient lines (Figure 4B, left), all of which had lost the ability to grow under standard media conditions, but were able to grow in media supplemented with 10 mM Mg^{2+} (Figure 4B, right and our unpublished data).

The ability of Mg^{2+} supplementation to complement TRPM7-deficiency produced through two distinct genetic approaches suggested that TRPM7 is involved in regulation of cellular Mg^{2+} homeostasis. As an initial
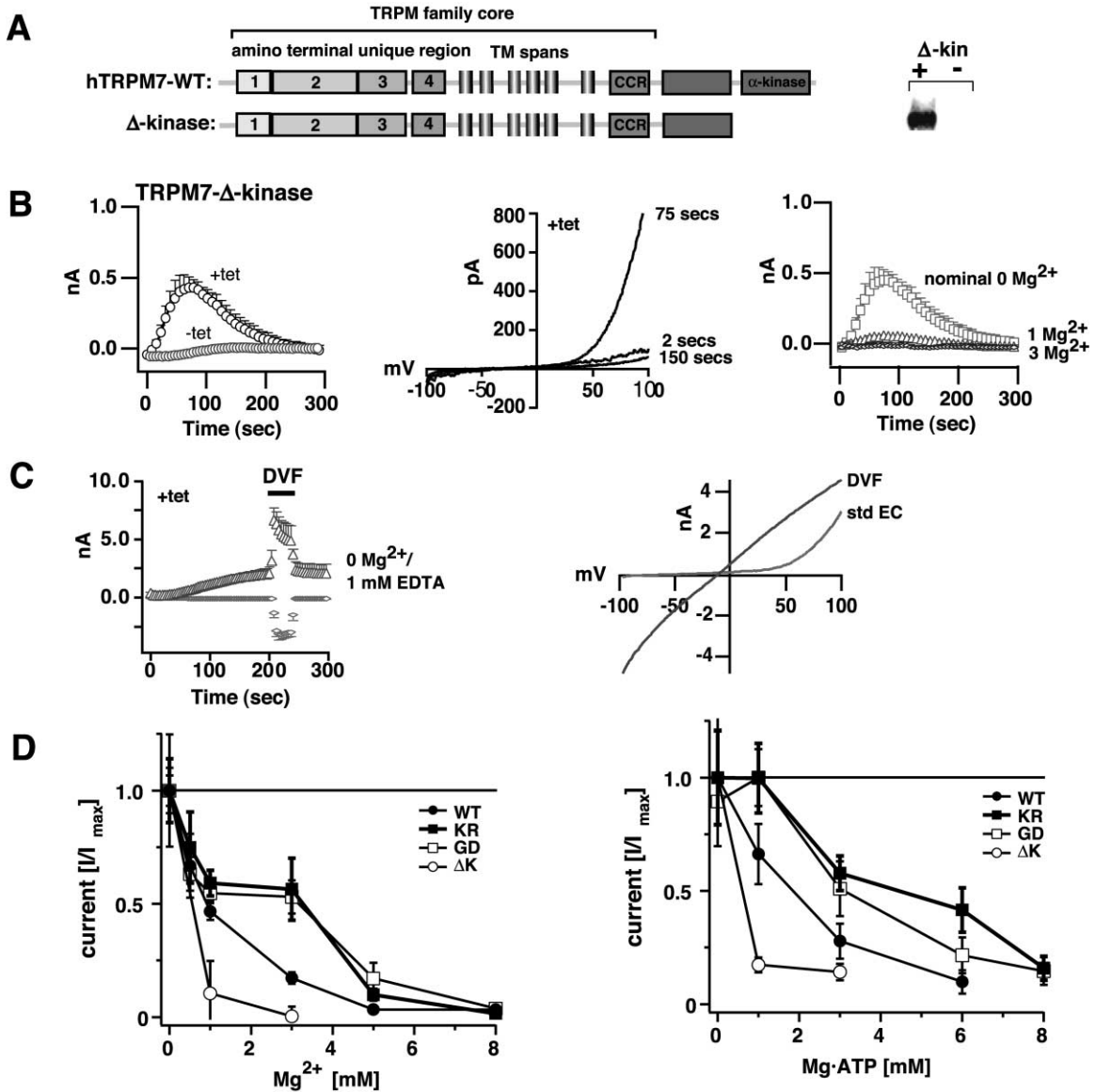
Figure 3. Analysis of Mg²⁺-Mediated Regulation of TRPM7-Δ-Kinase

(A) Left: schematic of TRPM7-Δ-kinase (TRPM7-ΔK or ΔK) in relation to WT TRPM7. Right: anti-HA immunoblot analysis of HEK-293 cells with doxycycline-regulated expression of human HA-TRPM7-Δ-kinase. Abbreviations: +, doxycycline treated; −, untreated.

(B) Left: whole-cell patch clamp analysis of currents produced on break in with nominal 0 Mg²⁺ pipette solution. Plots represents n = 5 experiments in each case. Middle: IV curves at the indicated times from a representative experiment. Right: whole-cell patch clamp analysis of Mg²⁺ suppression of HA-TRPM7-Δ-kinase. Pipette solutions contained the indicated concentrations of free Mg²⁺. Plots represent n = 5, 3, 3 experiments (0, 1, 3 mm Mg²⁺, respectively). Note the 0 Mg²⁺ curve is the same as in (B), left.

(C) Left: Δ-kinase currents approach WT-TRPM7 when intracellular Mg²⁺ is clamped to 0 by 1 mM EDTA addition to standard intracellular solution. DVF = extracellular perfusion with divalent free solution. Right: I/V relationships for Δ-kinase with standard extracellular solution (std EC) and divalent free solutions (DVF). Note large current flow and linearization of I/V curve on perfusion with DVF solution.

(D) Dose-response curves for Mg²⁺ suppression (left) and Mg·ATP suppression (right) of whole-cell currents carried by the various TRPM7 constructs. Data represent peak whole-cell currents at the indicated Mg²⁺ and Mg·ATP concentrations normalized to the maximum whole-cell current attained at 0 mM Mg·ATP. Free Mg²⁺ levels were fixed to 500 μM at all Mg·ATP concentrations. Δ-kinase data were collected 22–26 hr after tetracycline induction.

step toward understanding what its role might be, we used one of the stably TRPM7-deficient cell lines (designated KO cells) to compare total cellular Mg²⁺ under standard growth conditions with that of the same cells grown in 10 mM supplemental Mg²⁺ (Figure 4C, left). After 24 hr of growth under standard conditions, KO cells exhibited profound decreases in total cellular Mg²⁺ relative to growth with supplemental Mg²⁺. While we consistently observed this degree of depletion in total Mg²⁺ at these time points in KO cells grown in regular media relative to KO cells grown with supplemental Mg²⁺ or WT DT-40 cells grown in either condition, the magni-
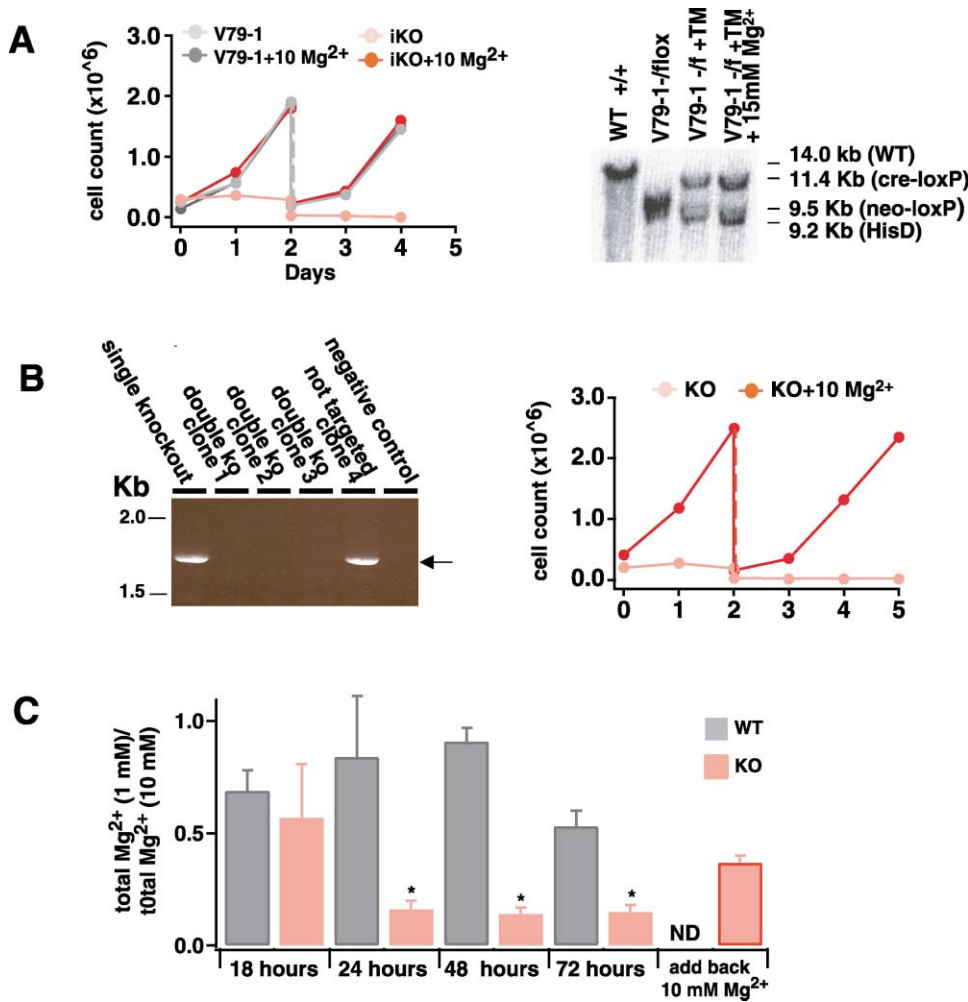
Figure 4. Complementation by Mg²⁺ Supplementation and Characterization of the TRPM7⁻/⁻ (KO) Phenotype

(A) Left: growth curves of the V79-1 knockout clone before (V79-1, gray symbols) and after (iKO, red symbols) inducible disruption of the second TRPM7 allele, and with (dark symbols) and without (light symbols) 10 mM MgSO₄ supplementation. Dotted lines indicate splitting down of cells. Right: Southern blot analysis of XbaI digested genomic DNA from WT DT40 and the inducible TRPM7 knockout clone V79-1, before and after tamoxifen (TM)-induced disruption of the second TRPM7 allele, with or without addition of 15 mM MgSO₄ into the medium. Analysis of TRPM7 expression by RT-PCR of a 1.8 kb fragment of chicken TRPM7 cDNA was also performed in the V79-1 TRPM7 inducible deletion cell line before disruption of the second allele, after disruption (+TM), and after disruption of the second allele and growth in medium supplemented with 15 mM MgSO₄; this analysis demonstrated complete absence of the TRPM7 transcript after tamoxifen treatment (not shown).

(B) Left: analysis of TRPM7 expression by RT-PCR of a 1.8 kb fragment of chicken TRPM7 cDNA in several TRPM7 knockout cell lines produced using a standard knockout approach (lanes 2–4) with selection in the presence of 10 mM MgSO₄, two positive control cell lines (lane 1, the single allele knockout parental line; lane 5, a resistant clone which was able to grow without supplemental Mg²⁺), and a negative control (lane 6, no template). Right: growth curves of one KO cell line clone with (dark red line/symbols) and without (light red line and symbols) 10 mM supplemental MgSO₄. Similar results were observed for several clones (not shown). Dotted line between two points on the same day indicates splitting down of cells.

(C) KO cells have reduced total cellular Mg²⁺ after growth in standard media. Bars represent the total cellular Mg²⁺ of cells grown in regular media normalized to that of cells grown in media with 15 mM supplemental Mg²⁺. For add-back conditions, KO cells grown in standard media for 72 hr were placed back in media with 15 mM supplemental MgSO₄ for 48 hr and then assayed for total cellular Mg²⁺. These values were then normalized to the average total cellular Mg²⁺ of KO cells grown in 15 mM MgSO₄ for 72 hr. Asterisk indicates that reductions in ratio of knockout cells relative to WT cells at 24, 48, and 72 hr are statistically significant at p < 0.01.

tude of the decrease observed in these experiments should be interpreted cautiously, as KO cells begin to die over a 24–72 hr frame after being placed in standard media such that a portion of any decrease in total Mg²⁺ measured at these times could potentially be due to loss of Mg²⁺ from nonviable cells. To attempt to account for this problem, total Mg²⁺ was conservatively normal-

ized on a per-viable-cell basis, using a combination of visual inspection and trypan blue staining. The viability of the cells present at the later time points is also supported by the ability of 10 mM Mg²⁺ supplementation to substantially replenish total cellular Mg²⁺ (Figure 4C, add back category of left panel) and support renewed cell growth of KO cells after 48–72 hr of existence in

standard media (data not shown). However, as the existence of cells that are nonviable yet look normal and exclude trypan blue is a formal possibility, we cannot exclude that a fraction of the measured decrease in total Mg^{2+} might be due to loss of Mg^{2+} due to impending death. An additional important point is that after existing in nonsupplemented media for 48–72 hr, KO cells appear smaller than WT DT-40 cells or KO cells which have been grown in Mg^{2+}-supplemented media, suggesting that a portion of the observed decrease in total Mg^{2+} per cell is due to a contraction of cytosol occurring for unknown reasons.

Characterization of Mg Homeostasis and Growth Phenotype in TRPM7-Deficient Cells Complemented with Heterologous WT, K1648R, and ΔK Channels

If TRPM7 indeed has a critical role as a Mg^{2+} uptake pathway and its kinase and channel domains are functionally coupled, KO cells expressing kinase domain mutant channels with altered Mg^{2+} suppression phenotypes would be expected to exhibit evidence of altered growth and Mg^{2+} homeostasis. In order to test these predictions, we attempted to heterologously express WT and mutant TRPM7 channels in our V79-1 cell line; however, despite repeated attempts, we were unable to produce any channel-expressing V79-1 lines for unclear reasons (>10 separate transfections failed to produced any expressing clones). Therefore, we created a new TRPM7-deficient DT-40 line by knocking out the second TRPM7 allele in a TRPM7-heterozygote DT-40 line expressing a bacterial tetracycline repressor protein. Retransfection of this line with HA-tagged WT TRPM7, TRPM7-K1648R, and TRPM7-ΔK channels under control of a tetracycline-regulated promotor was successful, and clones expressing similar levels of each respective channel type were chosen for further characterization (Figure 5A, left and right, henceforth these lines are designated cWT, cKR, and cΔK to indicate that they are KO cells complemented with the respective channel).

Using these cell lines, we analyzed the capacity of each channel to support cell viability and proliferation in standard media, and each channel's effect on total cellular Mg^{2+}. As shown in Figure 5B (top left, top right, and bottom left), when grown in the absence of doxycycline in standard media, the complemented cell lines exhibit growth characteristics distinct from the KO cells: the cWT and cKR cell lines do not die; their growth simply slows down to a lower rate, while the cΔK cells die but do so over a more prolonged time course than KO cells (light red curves and data not shown). Based on this, we infer that these cell lines have some degree of basal expression of their respective transfected channels, presumably due to a small degree of promotor leakiness. In contrast, when grown in the presence of doxycycline, the cWT and cKR lines are viable and proliferate at rates indistinguishable from WT cells, while the cΔK line is viable but only regains the ability to proliferate very slowly. These growth characteristics are important to consider when interpreting the total cellular Mg^{2+} of the cWT, cKR, and cΔK cell lines (Figure 5B, bottom right). All three cell lines are significantly Mg^{2+} deficient when grown in the absence of doxycycline treatment

for 48 hr (designated by an asterisk, $p < 0.01$ including Bonferonni correction for multiple comparisons), although not to the same degree as untransfected KO cells, consistent with their altered growth and viability characteristics under these conditions. However, while treatment of doxycycline to induce cWT and cKR channel expression is able to restore the total cellular Mg of cWT and cKR cell lines to normal levels, induction of cΔK channel expression left cΔK cells significantly Mg^{2+} deficient ($p < 0.01$, designated by a double asterisk), consistent with the inability of these cells to resume a normal rate of growth. The correspondence between the viability and growth phenotype, total cellular Mg levels, and Mg^{2+}-suppression phenotype of the respective channels is striking: expression of channels exhibiting normal or lower Mg^{2+} suppression (e.g., WT and KR channels) allows sufficient Mg^{2+} entry to support total cellular Mg levels and normal cell division. Conversely, the ΔK channel, which is more sensitive to Mg^{2+} suppression and would therefore shut off sooner than the other channels, is only able to support a low level of total cellular Mg and a reduced rate of cell division.

Discussion

The model of TRPM7 function which has been previously put forth is that TRPM7 acts as a Na^+ and Ca^{2+} permeant channel whose channel activity is somehow dependent on the phosphotransferase activity of its intrinsic kinase domain (Runnels et al., 2001). However, such a model is not consistent with our observations that mutant TRPM7 channels essentially devoid of detectable phosphotransferase activity exhibit sustained channel activation comparable to WT channels under conditions of nominal zero intracellular free [Mg^{2+}]. Future models of TRPM7 function will need to explain this observation, as well as incorporate a functional coupling between the channel and kinase domains, account for the ability of supplemental Mg^{2+} to complement the growth defect associated with TRPM7 deficiency, and account for the correlation between the Mg^{2+} suppression phenotype of mutant channels and their ability to complement growth and Mg^{2+} homeostasis of TRPM7-deficient cells. Based on these observations, we propose that TRPM7 acts as a primarily Mg^{2+}-permeant ion channel, which acts as a cellular Mg^{2+} uptake mechanism, and that Mg^{2+}-dependent channel suppression (and hence Mg^{2+} uptake) is modulated through a functional coupling between the channel gating mechanism and the kinase domain.

While our results provide insight into the cell biological role of TRPM7's channel function, the physiologic and molecular targets of the phosphotransferase activity of TRPM7 remain unidentified. TRPM7's ability to sense cytosolic Mg^{2+}/Mg·ATP levels and transduce this information into altered TRPM7 channel activity is clearly influenced by the kinase domain, but the divergent phenotypes of the phosphotransferase-activity-deficient point mutant channels and the ΔK channel indicate that the kinase domain's influence is not dependent on TRPM7 autophosphorylation. Furthermore, the kinase domain cannot itself be the "sensor" domain that closes the channel in response to increased Mg^{2+}/Mg·ATP lev-
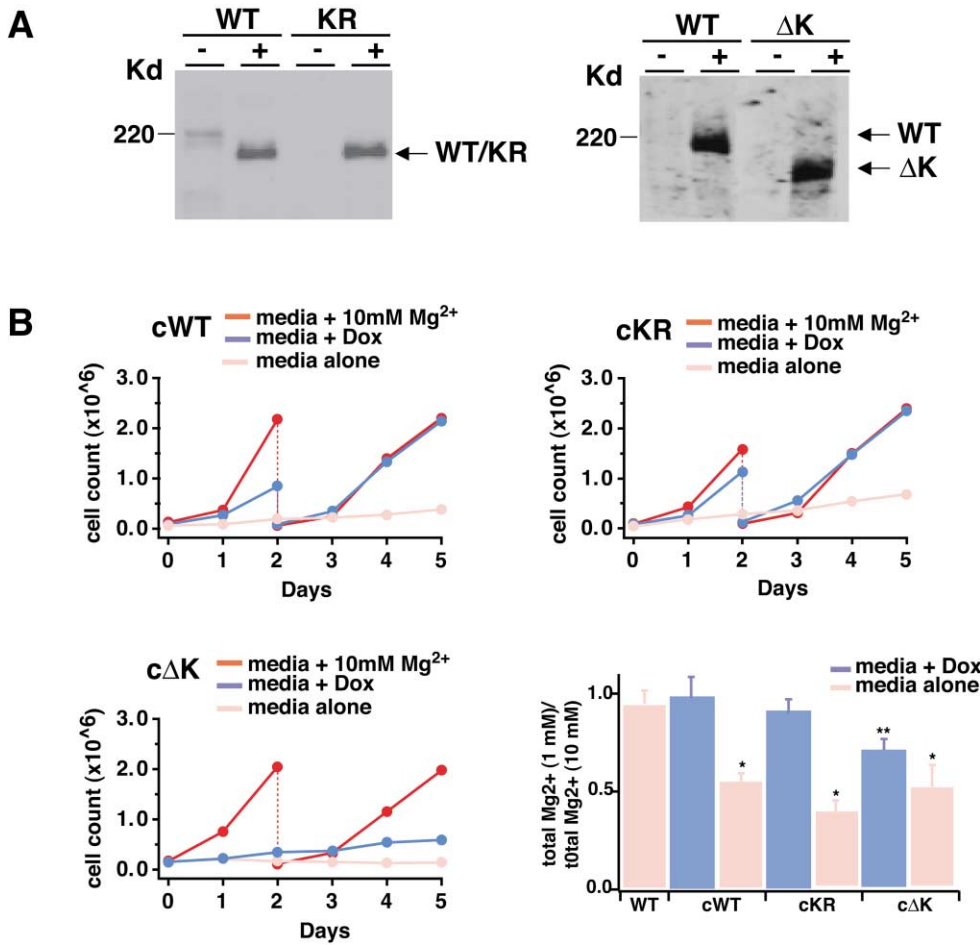
A

B

Figure 5. Compensation of the TRPM7$^{-/-}$ Lethal Phenotype by WT and Mutant TRPM7 Channels

(A) Left: analysis of inducible TRPM7 channel expression in DT-40 KO cell lines expressing HA-tagged TRPM7-WT (cWT cell line) and TRPM7-K1648R (cKR cell line). Right: analysis of inducible TRPM7 channel expression in DT-40 KO cell lines expressing HA-tagged TRPM7-WT (cWT cell line) and TRPM7-ΔK (cΔK cell line). Equal numbers of cells from the respective cell lines were analyzed by Western immunoblotting with anti-HA antibody before and after doxycycline treatment.

(B) Top left, top right, and bottom left: growth curves of cWT, cKR, and cΔK cells, respectively, in the presence of media alone (light red), media plus doxycycline (blue), and media plus 10 mM MgSO$_4$ (red). Dotted line between two points on the same day indicates splitting down of cells. Note that the induced cΔK cells were not split until day 7, while induced cWT and cKR cells required splitting every 2–3 days. Bottom right: Analysis of total cellular Mg^{2+} in cWT−, cKR−, and cΔK cell lines grown in standard media with (blue) and without (light red) doxycycline treatment for 48 hr. Bars represent the total cellular Mg^{2+} of cells grown in regular media normalized to that of cells grown in 15 mM supplemental MgSO$_4$. Numbers for WT and cΔK cells are averages of n = 8 replicates; Numbers for the cWT and cKR cells are averages of n = 4 replicates. Asterisk indicates that reductions of ratio in the uninduced cells of each type relative to wild-type cells are statistically significant at p < 0.01, including Bonferroni correction for multiple comparisons. Double asterisk (**) indicates that reduction of ratio in induced cΔK compared to WT cells is statistically significant at p < 0.01.

els, as Δ-kinase channels exhibit intact (albeit altered) Mg^{2+}/Mg·ATP suppression. While it is conceivable that the phosphotransferase activity of the kinase domain is vestigial and has no distinct function, this seems unlikely given the conservation of the enzymatic activity of the kinase domain despite significant divergence of its amino acid sequence from other members of the α-kinase family (Ryazanov, 2002). A model that we presently favor is that TRPM7's phosphotransferase activity is required to phosphorylate as yet unidentified molecular targets for the purpose of providing "real time" information to these targets regarding alterations in cytosolic Mg^{2+}/Mg·ATP levels, channel state, and/or Mg^{2+} entry. This possibility is supported by the coordinated changes

in phosphotransferase activity and ion flow observed in response to changes in free [Mg^{2+}] for WT TRPM7 in Figure 1. However, if the kinase domain has an information transfer function of importance to cell function, how are KR phosphotransferase-activity-deficient channels able to complement the viability and growth defects of TRPM7-deficient cells as well as WT channels? The ability of high level Mg^{2+} supplementation to support normal cell proliferation in TRPM7-deficient cells clearly demonstrates that as long as sufficient Mg^{2+} entry occurs, cellular Mg^{2+} homeostasis mechanisms (presumably involving sequestration/mobilization from intracellular stores and/or Mg^{2+} export) are able to maintain a sufficient degree of cellular Mg^{2+} homeostasis for cell

proliferation to occur in the absence of all TRPM7 function(s). Based on this observation, the increased rate of Mg^{2+} entry in K1648R channel-expressing cells could support cell growth in the same manner that 10 mM Mg^{2+} supplementation of the media does in the complete absence of TRPM7—by providing an enhanced, albeit dysregulated, entry of Mg^{2+}. Whether the absence of TRPM7 phosphotransferase activity in K1648R-expressing cells is associated with a dysregulation of other cell biological phenomena due to the loss of information transfer downstream from TRPM7 is an intriguing topic for future investigation.

In summary, our results provide insight into the functional relationship between TRPM7's channel and kinase domains and indicate that a central cell biological role of TRPM7 is to act as a Mg^{2+} uptake mechanism involved in the homeostatic regulation of vertebrate cellular Mg^{2+}. The discovery of such a role for TRPM7 is an important step toward understanding vertebrate Mg^{2+} regulatory mechanisms at the molecular level and has the significant implication that these mechanisms are likely to be substantially different from those found in unicellular eukaryotes, plants, or bacteria, where the known Mg^{2+} uptake pathways utilize transport proteins without kinase domains or other obvious homology to TRPM7 (Bui et al., 1999; Graschopf et al., 2001; Gregan et al., 2001; Li et al., 2001; Romani and Scarpa, 2000; Smith and Maguire, 1998).

Experimental Procedures

Cloning, Expression, and Analysis of Human TRPM7 and TRPM7 Mutants in Mammalian Cells
The methods for isolation, cloning, and expression of hTRPM7 full-length channel (accession number human TRPM7: AY 032950) in mammalian cells are identical to those previously described (see supplemental information for Nadler et al., 2001, at http://www.nature.com/nature/journal/v411/n6837/suppinfo/411590a0.html), except that an N-terminal HA-tag was used instead of a FLAG tag for production of the expression construct. Cloning of TRPM7 mutants in the expression vector was performed in the identical manner as the WT's—the mutants were generated by site-directed mutagenesis using the QuickChange kit from Stratagene (following the standard protocol), and the presence of the correct mutation and lack of other mutations was confirmed by sequencing of the entire construct in each case. Figure 2 gives detailed information about the introduced mutations. The stably transfected 293-HEK cells (expressing WT hTRPM7 and hTRPM7 mutants) were maintained and induced using doxycycline as described earlier (Nadler et al., 2001). Immunoprecipitations and Western blotting: anti-HA immunoprecipitations were performed from lysates (the phosphatase inhibitor Calyculin A (10 nM) was added to the lysis buffer for phosphorylation experiments) of 10^7 HEK-293 cells. Immunoprecipitated proteins were washed three times with lysis buffer, separated by SDS-PAGE using 6% polyacrylamide gels, transferred to a PVDF membrane, and analyzed by anti-HA immunoblotting or by anti-P-Thr-immunoblotting—blots were sometimes reprobed after stripping. All procedures used standard methods.

Electrophysiology
HEK-293 cells transfected with the HA-human TRPM7 or indicated mutants subcloned into the pCDNA4/TO plasmid were grown on glass coverslips with DMEM medium supplemented with 10% fetal bovine serum, blasticidin (5 μg/ml), and zeocin (0.4 mg/ml). TRPM7 expression was induced by adding 100–1000 ng/ml doxycycline to the culture medium. Whole-cell patch-clamp experiments were performed at 21°C–25°C 18–24 hr postinduction using cells grown on glass coverslips and kept in a standard modified Ringer's solution of the following composition: 145 mM NaCl, 2.8 mM KCl, 10 mM

CsCl, 1 mM $CaCl_2$, 2 mM $MgCl_2$, 10 mM glucose, and 10 mM Hepes·NaOH (pH 7.2). Intracellular pipette-filling solutions contained 145 mM Cs-glutamate, 8 mM NaCl, $MgCl_2$ and Mg·ATP as indicated, 10 mM Cs-EGTA, and 10 mM Hepes·CsOH [pH 7.2]. Free $[Mg^{2+}]i$ was calculated using WebMaxC2.10 (http://www.stanford.edu/cpatton/webmaxc2.htm) using a temperature of 24°C (pH 7.2), and ionic strength of 0.16. High-resolution current recordings were acquired by a computer-based patch-clamp amplifier system (EPC-9, HEKA, Lambrecht, Germany). Immediately following establishment of the whole-cell configuration, voltage ramps of 50 ms duration spanning the voltage range of −100 to +100 mV were delivered from a holding potential of 0 mV at a rate of 0.5 Hz over a period of 300–400 s. All voltages were corrected for a liquid junction potential of 10 mV between external and internal solutions when internal solutions contained glutamate. Currents were filtered at 2.3 kHz and digitized at 100 μs intervals. Capacitive currents and series resistance were determined and corrected before each voltage ramp using the automatic capacitance compensation of the EPC-9. The low-resolution temporal development of currents at a given potential was extracted from individual ramp current records by measuring the current amplitudes at voltages of −80 mV or +80 mV. Note that outward and inward currents were altered in analogous fashion for each of the various hTRPM7 mutants and solution manipulations. The outward currents are reported for presentation purposes because of their larger magnitude relative to background and unequivocal correlation with TRPM7 activation.

DT-40 Cell Line Construction and Culture
The DT-40 cell line allowing inducible deletion of TRPM7 was previously described (Nadler et al., 2001), and was based on the inducible deletion system from Reth and colleagues (Zhang et al., 1998). Their culture and induction of deletion were all performed as previously described (Nadler et al., 2001). Complementation studies were performed with $MgCl_2$, $MgSO_4$, $MnCl_2$, $ZnSO_4$, and $CaCl_2$. Each was examined at concentrations of 1, 3, 5, 20, and 50 mM. Only Mg^{2+}-containing salts complemented, and there was no difference between $MgSO_4$ and $MgCl_2$.

TRPM7-KO cell lines in a WT DT-40 background and in a DT-40 parental cell line expressing the tetracycline transcriptional suppressor using pCDNA6/TR (Invitrogen) were constructed using a standard targeting approach identical to that utilized to delete the second allele of the V79-1 inducible deletion cell line (Nadler et al., 2001). All TRPM7-deficient cell lines behaved similarly in terms of cell growth, and all behaved nearly identically to the V79-1 inducible deletion line, with the exception that the V79-1 line appeared to have reduced TRPM7 function prior to Cre-mediated destruction of its remaining functioning allele, consistent with its floxed TRPM7 allele acting as a hypomorph. The TRPM7-deficient cell line expressing the tet suppressor protein was subsequently retransfected with constructs in pcDNA4/TO (Invitrogen) encoding HA-tagged TRPM7-WT (WT), TRPM7-K1648R (KR) channels, and TRPM7-Δkinase (Δk) channels, and two lines with the relatively matched inducible expression as assessed by anti-HA immunoblotting were chosen for further analysis.

In Vitro and In Vivo Phosphorylation Assays of hTRPM7
For in vivo assays, anti-HA immunprecipitates were run out on SDS-PAGE gels and analyzed by anti-phosphothreonine immunoblotting. Conditions tested included basal, stimulation with thrombin, stimulation with carbachol, and treatment with A23187 in the presence of high (15 mM) and low (0 mM) Mg., For in vitro assays, hTRPM7 was immunoprecipated with anti-HA, and beads were incubated in a total volume of 40 μl reaction buffer A (50 mM Tris-HCl, 0.1 [v/v] β-mercaptoethanol, 10 nM Calyculin A, 100 mM Mg-ATP containing different magnesium acetate concentrations) or in reaction buffer B (50 mM HEPES-KOH [pH 7.2]), 0.1 (v/v) β-mercaptoethanol, 10 nM Calyculin A using different concentrations of $MgCl_2$, and Mg·ATP. EDTA was added as necessary to clamp free $[Mg^{2+}]$ to the indicated concentrations as calculated using WebMaxC2.1. Phosphorylation was analyzed after gel electrophoresis by anti-P-Thr-immunoblotting (using anti-Phospho-Threonine antibody from CellSignaling cat. 9381). The pH was kept constant in all phosphorylation reactions at 7.2.

Total Cellular Magnesium Measurements

For measurements of total cellular Mg^{2+}, cells were grown in RPMI supplemented with either 10% FBS and 1% chicken serum or both types of sera plus 10 mM $MgSO_4$. WT DT-40 cells, the parental V79-1 cell line, and the cWT- and cKR-complemented cells grow apparently normally in the RPMI/10%FBS/1% chicken serum, while TRPM7 KO cells go into immediate growth arrest in this media and cΔK cells go into growth arrest after 48 hr or so. For total Mg^{2+} assays, each culture was started with 2×10^6 cells in 10 mls of media and allowed to grow in the indicated media for the indicated times. Total Mg^{2+} was extracted at the indicated times by treatment of cells with 5% trichloroacetic acid (TCA), and the extractate was assayed using atomic absorption spectrophotometry. Normalization on a per-cell basis was performed using a combination of visual counts of morphologically normal appearing cells and trypan blue staining. Protein concentrations of lysates were also determined and generally correlated well with the results of the cell counts (not shown). Differences between cells grown in 10 mM and 1 mM Mg^{2+} do not reflect carryover of media Mg^{2+}, as growth of cells in 1 mM Mg^{2+} followed by resuspension in 10 mM Mg^{2+} supplemented media and then washing, and assay as usual showed no detectable carryover.

Acknowledgments

References

Bui, D.M., Gregan, J., Jarosch, E., Ragnini, A., and Schweyen, R.J. (1999). The bacterial magnesium transporter CorA can functionally substitute for its putative homologue Mrs2p in the yeast inner mitochondrial membrane. J. Biol. Chem. *274*, 20438–20443.

Clapham, D.E., Runnels, L.W., and Strubing, C. (2001). The TRP ion channel family. Nat. Rev. Neurosci. *2*, 387–396.

Elliott, A.C. (2001). Recent developments in non-excitable cell calcium entry. Cell Calcium *30*, 73–93.

Graschopf, A., Stadler, J.A., Hoellerer, M.K., Eder, S., Sieghardt, M., Kohlwein, S.D., and Schweyen, R.J. (2001). The yeast plasma membrane protein Alr1 controls Mg2+ homeostasis and is subject to Mg2+-dependent control of its synthesis and degradation. J. Biol. Chem. *276*, 16216–16222.

Gregan, J., Bui, D.M., Pillich, R., Fink, M., Zsurka, G., and Schweyen, R.J. (2001). The mitochondrial inner membrane protein Lpe10p, a homologue of Mrs2p, is essential for magnesium homeostasis and group II intron splicing in yeast. Mol. Gen. Genet. *264*, 773–781.

Hara, Y., Wakamori, M., Ishii, M., Maeno, E., Nishida, M., Yoshida, T., Yamada, H., Shimizu, S., Mori, E., Kudoh, J., et al. (2002). LTRPC2 Ca2+-permeable channel activated by changes in redox status confers susceptibility to cell death. Mol. Cell *9*, 163–173.

Harteneck, C., Plant, T.D., and Schultz, G. (2000). From worm to man: three subfamilies of TRP channels. Trends Neurosci. *23*, 159–166.

Hermosura, M.C., Monteilh-Zoller, M.K., Scharenberg, A.M., Penner, R., and Fleig, A. (2002). Dissociation of the store-operated calcium current I(CRAC) and the Mg-nucleotide-regulated metal ion current MagNuM. J. Physiol. *539*, 445–458.

Hofmann, T., Schaefer, M., Schultz, G., and Gudermann, T. (2000). Transient receptor potential channels as molecular substrates of receptor-mediated cation entry. J. Mol. Med. *78*, 14–25.

Li, L., Tutone, A.F., Drummond, R.S., Gardner, R.C., and Luan, S. (2001). A novel family of magnesium transport genes in Arabidopsis. Plant Cell *13*, 2761–2775.

MacDiarmid, C.W., and Gardner, R.C. (1998). Overexpression of the Saccharomyces cerevisiae magnesium transport system confers resistance to aluminum ion. J. Biol. Chem. *273*, 1727–1732.

Monteilh-Zoller, M.K., Hemosura, M.C., Nadler, J.S., Scharenberg, A.M., Penner, R., and Fleig, A. (2003). TRPM7 provides an ion channel mechanism for cellular entry of trace metal ions. J. Physiol. *121*, 1–13.

Montell, C., Birnbaumer, L., and Flockerzi, V. (2002). The TRP channels, a remarkably functional family. Cell *108*, 595–598.

Nadler, M.J.S., Hermosura, M.C., Inabe, K., Perraud, A.-L., Zhu, Q., Stokes, A., Kurosaki, T., Kinet, J.-P., Penner, R., Scharenberg, A.M., and Fleig, A. (2001). LTRPC7 is a Mg·ATP-regulated divalent cation channel required for cell viability. Nature *411*, 590–595.

Perraud, A.L., Fleig, A., Dunn, C.A., Bagley, L.A., Launay, P., Schmitz, C., Stokes, A.J., Zhu, Q., Bessman, M.J., Penner, R., et al. (2001). ADP-ribose gating of the calcium-permeable LTRPC2 channel revealed by Nudix motif homology. Nature *411*, 595–599.

Perraud, A.-L., Schmitz, C., and Scharenberg, A.M. (2003). TRPM2: from gene to biological function. Cell Calcium *382*, 1–13.

Romani, A.M., and Scarpa, A. (2000). Regulation of cellular magnesium. Front. Biosci. *5*, D720–734.

Runnels, L.W., Yue, L., and Clapham, D.E. (2001). TRP-PLIK, a bifunctional protein with kinase and ion channel activities. Science *291*, 1043–1047.

Runnels, L.W., Yue, L., and Clapham, D.E. (2002). The TRPM7 channel is inactivated by PIP(2) hydrolysis. Nat. Cell Biol. *4*, 329–336.

Ryazanov, A.G. (2002). Elongation factor-2 kinase and its newly discovered relatives. FEBS Lett. *514*, 26–29.

Sano, Y., Inamura, K., Miyake, A., Mochizuki, S., Yokoi, H., Matsushime, H., and Furuichi, K. (2001). Immunocyte Ca2+ influx system mediated by LTRPC2. Science *293*, 1327–1330.

Smith, R.L., and Maguire, M.E. (1998). Microbial magnesium transport: unusual transporters searching for identity. Mol. Microbiol. *28*, 217–226.

Vennekens, R., Voets, T., Bindels, R.J., Droogmans, G., and Nilius, B. (2002). Current understanding of mammalian TRP homologues. Cell Calcium *31*, 253–264.

Wehage, E., Eisfeld, J., Heiner, I., Jungling, E., Zitt, C., and Luckhoff, A. (2002). Activation of the cation channel long transient receptor potential channel 2 (LTRPC2) by hydrogen peroxide. A splice variant reveals a mode of activation independent of ADP-ribose. J. Biol. Chem. *277*, 23150–23156.

Yamaguchi, H., Matsushita, M., Nairn, A.C., and Kuriyan, J. (2001). Crystal structure of the atypical protein kinase domain of a TRP channel with phosphotransferase activity. Mol. Cell *7*, 1047–1057.

Zhang, Y., Wienands, J., Zurn, C., and Reth, M. (1998). Induction of the antigen receptor expression on B lymphocytes results in rapid competence for signaling of SLP-65 and Syk. EMBO J. *17*, 7304–7310.